

Transit Times in Fire Plumes and Ceiling Layers

Tamanini F.

FM Global, Research Division, Norwood, Massachusetts, USA

francesco.tamanini@fmglobal.com

ABSTRACT

Previous work has introduced a method to infer the convective heat release rate (HRR) of a fire from the gas temperatures measured in the thermal layer near a ceiling. The modeling approach gave no consideration to the impact of flow transport on the HRR estimates obtained from measurements made at different distances from the axis of the fire plume. This omission introduces errors in the evaluation of growth rates for rapidly developing fires. The work described in the paper enhances the earlier model by implementing standard plume and ceiling layer correlations to calculate the gas travel time in the fire plume and in the ceiling layer. The estimated travel times are then used to correct the measurement time to the time of the fire. Examples are provided to demonstrate how the correction reduces the errors in fire growth rate, which are encountered when the characteristic time of the growth is of the order of or smaller than the gas travel time to the point where the temperature measurement is made. The correction has been implemented in an engineering tool, which is used internally for fire test data analyses.

KEYWORDS: Transit time, fire plume, ceiling layer, large-scale fire tests.

NOMENCLATURE

D	pool diameter (m)	z	vertical distance (m)
H	ceiling distance above fuel array (m)	z_0	virtual source height (m)
n	number of tiers in fuel array (-)		
\dot{Q}_c	convective heat release rate (kW)	Greek	
r	radial distance along ceiling (m)	α_N	time step fraction (-)
r_{tr}	radius of plume turning region (m)	γ	relaxation factor (-)
s	travel path length (m)	Δt	time interval (s)
t	time (s)	ΔT	temperature rise (K)
t_{TR}	transport time (s)	Subscripts	
T	temperature (K)	H	conditions at the ceiling
T_∞	ambient temperature (K)	lim	plume transition
u_m	peak ceiling layer velocity (m/s)	Superscripts	
u_0	peak fire plume velocity (m/s)	+	increasing HRR
V	average flow velocity (m/s)	-	decreasing HRR

BACKGROUND

A fire under an unconfined ceiling generates a thermal layer, the properties of which can be related through standard correlations to the geometry of the system (mainly ceiling height) and the heat release rate (HRR) characteristics of the fire (fuel array type/dimensions and convective HRR). Given this information, it is conceptually possible to solve the inverse problem, namely calculate

Proceedings of the Ninth International Seminar on Fire and Explosion Hazards (ISFEH9), pp. 596-607

Edited by Snegirev A., Liu N.A., Tamanini F., Bradley D., Molkov V., and Chaumeix N.

Published by St. Petersburg Polytechnic University Press

ISBN: 978-5-7422-6496-5 DOI: 10.18720/spbpu/2/k19-98

the convective HRR from the gas temperatures measured at the ceiling. This task was undertaken through work documented in an earlier paper [1] and was recently enhanced by an analysis [2], which has led to an improved set of correlations. A potential difficulty is encountered when this inverse method for calculating the convective HRR is applied to cases where the fire output changes rapidly. This becomes an issue when estimating fire growth rates or the rapid decrease in HRR at the end of a test (e.g., pool fires, or fast suppression), because of the finite amount of time needed by the flow induced by the fire to reach the location at which the gas temperature measurement is made. Furthermore, for a given geometry, this travel time depends on the HRR of the fire. The greater the HRR, the higher the gas velocity and the shorter the travel time. So, distance traveled and fire intensity are both important parameters. For a quasi-steady fire (one for which the characteristic time for a change in HRR is large relative to the flow travel time to the measurement location), the effect is small and reliable fire growth information can be obtained consistently from thermocouples at different distances from the fire axis. In many cases of practical interest, however, this condition is not satisfied and the error introduced by the effect cannot be neglected.

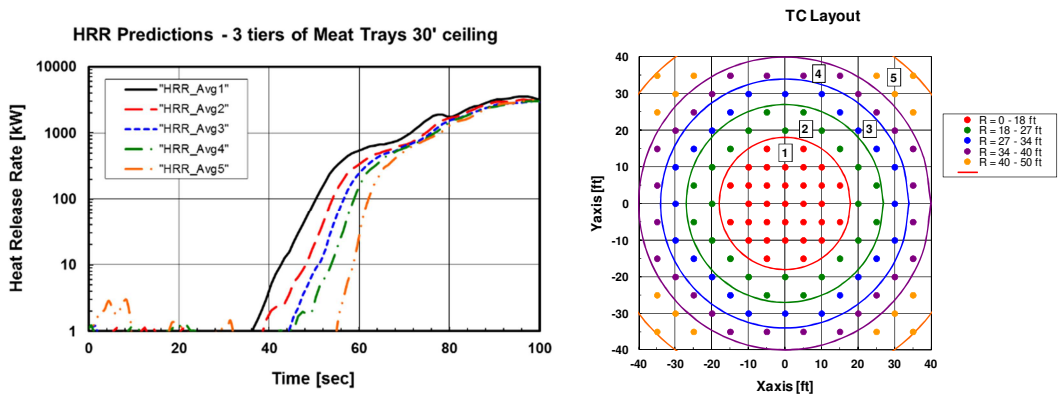


Fig. 2. Convective Heat Release Rate development inferred from thermocouple measurements during a fire test with three tiers (4.27-m [14-ft] high) of meat trays under a 9.1-m (30-ft) ceiling. Data presented as averages over the five zones indicated in the right side of the figure. Adapted from Ref. [1].

This issue had been identified and documented with fire test data (cf., Fig. 3 of Ref. [1]). A typical example of the error is given plot of Fig. 1, which shows a case from that reference with the HRR curves recalculated using the recently-developed improved correlations [2]. In the figure, the individual HRR estimates obtained from each of the 125 thermocouples installed under the ceiling are reported as averages over the five zones shown in the right side of the figure. As can be seen, the exponential rate of fire growth, represented in the semi-log plot by the slope of the line between approximately 10 and 500 kW, depends on the location of the thermocouples used for the calculations. The more distant TCs (cf., HRR_Avg5, corresponding to TCs at radii 12.2-15.2 m (40-50 ft) from the fire axis) imply a faster growth rate. This result is due to the fact that the flow information of a fire at the low end of the HRR range takes longer than that from a more intense fire to reach the measurement location. The effect, though still present, becomes less significant when the HRR is calculated using TCs at locations closer to the fire axis (e.g., HRR_Avg1).

The estimation of the delay between changes in the HRR of the fire and the time at which these changes manifest themselves a certain distance away has been tackled by previous work. In the case of Ref. [3], an analysis was done by assuming a power law growth of HRR in order to facilitate obtaining a solution for the flow conservation equations. The generality of this study was limited by the fact that only the transport in the fire plume was considered (no ceiling layer), as the issue tackled by the research was the time lag of measurements obtained using a fire products collector. The more recent work of Ref. [4] has included consideration of transport under a ceiling but has still

restricted itself to the case of power-law growing fires. The correction method presented here is not bound by this constraint as it applies to arbitrary HRR vs. time histories.

MODEL EQUATIONS

The formulas used in this analysis are those reported in the recent review of published correlations [2]. These equations provide relationships for the development of the profiles of gas velocity and temperature. Since the focus of the present analysis is on transport times, it will be assumed that the controlling factors for the propagation of information on HRR changes at the source are the peak velocities in the fire plume and in the ceiling layer. These velocities are functions of height (plume) and radial distance (layer). Only the formulas that are necessary for the travel time calculation will be repeated here. For the complete set, the interested reader is referred to the cited reference [2].

Fire Plume

Based on the above assumptions, the travel time in the fire plume from the virtual source to the ceiling level can be calculated as:

$$t_{TR} = \int_{z_0}^H \frac{dz}{u_0} \quad (1)$$

The expressions for peak velocity as a function of position in the fire plume are given by the following equations for the two cases of the flame and the non-reacting portion of the flow, as determined by the height, z_{lim} , which defines the transition between those two regions:

$$u_0 \text{ [m/s]} = 7.225((z - z_0) \text{ [m]})^{1/2} \quad \text{for } z \leq z_{lim} \quad (2)$$

$$u_0 \text{ [m/s]} = 1.179(\dot{Q}_c \text{ [kW]})^{1/3} ((z - z_0) \text{ [m]})^{-1/3} \quad \text{for } z > z_{lim} \quad (3)$$

Based on the above expressions, the travel time is then calculated from Eq. (1) yielding:

Case $H \leq z_{lim}$ (Continuous or highly intermittent flame impinging on the ceiling)

$$t_{TR} \text{ [sec]} = 0.2768((H - z_0) \text{ [m]})^{1/2} \quad (4)$$

by using Eq. (2) for u_0 , and

Case $H > z_{lim}$ (Moderately intermittent flame or non-reacting plume impinging on the ceiling)

$$t_{TR} \text{ [sec]} = 0.05830(\dot{Q}_c \text{ [kW]})^{1/5} + \frac{0.6361}{\dot{Q}_c^{1/3}}((H - z_0) \text{ [m]})^{4/3} \quad (5)$$

It should be noted that the two terms in Eq. (5) arise because the integral in Eq. (1) needs to be split in two parts: first from z_0 to z_{lim} and then from z_{lim} to H with u_0 given by Eqs. (2) and (3), respectively.

In terms of parameters at the point of transition between the two plume regions (reacting vs. non-reacting portion), the transit times can alternatively be written as:

$$t_{TR} = 2 \frac{(z_{lim} - z_0)^{1/2}}{u_{0,lim}} \cdot (H - z_0)^{1/2} \quad \text{for } H \leq z_{lim} \quad (6)$$

$$t_{TR} = 1.25 \cdot \frac{z_{lim} - z_0}{u_{0,lim}} + 0.75 \cdot \frac{H - z_0}{u_{0,H}} \quad \text{for } H > z_{lim} . \quad (7)$$

In these two expressions, z_{lim} , $u_{0,lim}$, and $u_{0,H}$ are given by:

$$(z_{lim} - z_0)[m] = 0.1136(\dot{Q}_c [kW])^{2/5} , \quad (8)$$

$$u_{0,lim} [m/s] = 2.435(\dot{Q}_c [kW])^{1/5} , \quad (9)$$

$$u_{0,H} [m/s] = 1.179(\dot{Q}_c [kW])^{1/3} ((H - z_0)[m])^{-1/3} , \quad (10)$$

where \dot{Q}_c is the convective heat release rate [kW], and z_0 is the elevation of the virtual origin above the top of the fuel array [m]. The location of the virtual origin, z_0 , is calculated from:

$$z_0 [m] = z_{0,I} [m] + 0.095 \dot{Q}_c^{2/5} [kW] , \quad (11)$$

where

$$z_{0,I} [m] = -1.02D [m] \quad \text{for pool fires,} \quad (12)$$

$$z_{0,I} [m] = -0.5 \cdot 0.3048(5(n-1) + 4) \quad \text{for rack storage of } n \text{ tiers.} \quad (13)$$

CEILING LAYER

The travel time in the ceiling layer is calculated over the distance from the axis of the fire to the radial location of interest (as in the fire plume case, all formulas and their derivations are documented in Ref. [2]):

$$t_{TR} = \int_0^r \frac{dz}{u_m} , \quad (14)$$

where the peak horizontal velocity, u_m , is given by:

$$u_m = u_{0,H} , \quad \text{for } r/r_{tr} \leq 1 ,$$

$$u_m = u_{0,H} (r/r_{tr})^{-4/5} , \quad \text{for } r/r_{tr} > 1 \quad (15)$$

In the above equation, the peak plume velocity at the ceiling is (from Eqs. (2) and (3) with $z = H$):

$$u_{0,H} [m/s] = 7.225((H - z_0)[m])^{1/2} \quad \text{for } H \leq z_{lim} ,$$

$$u_{0,H} [m/s] = 1.179(\dot{Q}_c [kW])^{1/3} ((H - z_0)[m])^{-1/3} \quad \text{for } H > z_{lim} . \quad (16)$$

The radius of the turning region, r_{tr} , is calculated from:

$$r_{tr} = 0.162(1 + \Delta T_{0,H}/T_\infty)^{1/3} (H - z_0) + \max(0, z_{lim} - H) . \quad (17)$$

The temperature rise at the ceiling, which appears in Eq. (17), is given by:

$$\Delta T_{0,H}/T_{\infty} = 3.5 \quad \text{for } H \leq z_{lim},$$

$$\Delta T_{0,H}/T_{\infty} = 0.09325(\dot{Q}_c [\text{kW}])^{2/3} ((H - z_0)[\text{m}])^{-5/3} \quad \text{for } H > z_{lim}. \tag{18}$$

The transport time in the ceiling layer from the axis of the fire plume to the radial location of interest is then obtained by solving the integral in Eq. (14) yielding:

$$t_{TR} = \frac{r}{u_{0,H}} \quad \text{for } r \leq r_{ir} \tag{19}$$

and

$$t_{TR} = \frac{r_{ir}}{u_{0,H}} \left(\frac{4}{9} + \frac{5}{9} \left(\frac{r}{r_{ir}} \right)^{9/5} \right) \quad \text{for } r > r_{ir}. \tag{20}$$

TIME SHIFTING APPROACH

Case of prescribed HRR

For a defined geometry, if the HRR history is known, then values for gas temperature and velocity can be calculated at each target point as a function of time using the relevant steady-state correlations detailed in Ref. [2]. The calculated values then need to be shifted to account for the travel time from the fire virtual source to the target location. The time shift is implemented by using the following procedure, which is schematically shown in Fig. 2.

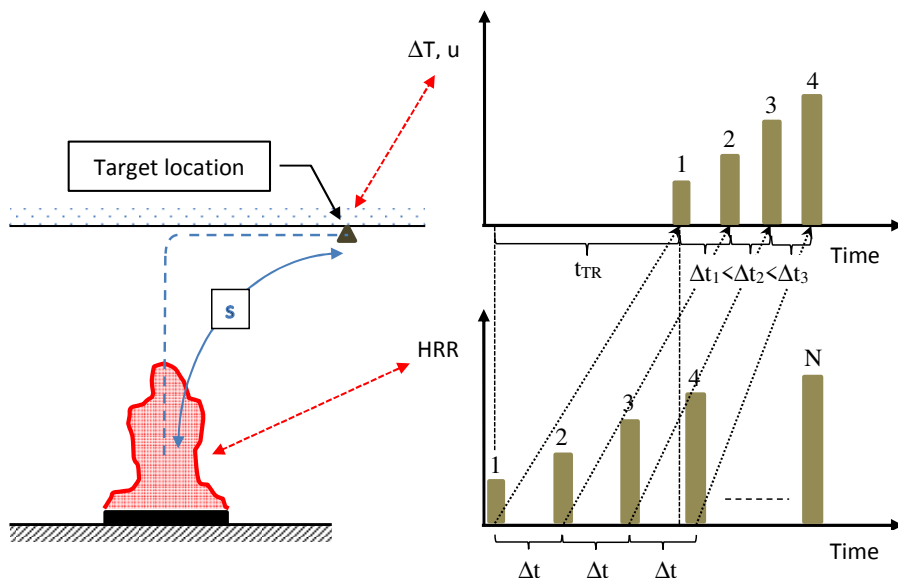


Fig.2. Travel of disturbances during fire growth. Target point is indicated by triangle.

For illustration purposes, the HRR time variation is visualized as a series of discrete steps, corresponding to increasing values $\dot{Q}_1, \dot{Q}_2, \dot{Q}_3$, etc. These HRR steps are separated by the constant time interval, Δt , which is defined by the data scan rate. Each HRR value has a corresponding value for the quantity of interest (gas temperature or velocity) at the target location, which is represented

in the top plot of the figure. As indicated, these values are assumed to be uniquely associated with the corresponding HRR through available correlations, though delayed by the transport time.

Again, for illustration purposes, it will be assumed that the flow characteristic associated with HRR value \dot{Q}_1 reaches the target location after a delay given by t_{TR} . As can be seen in the sketch of Fig. 2, during that time interval the HRR increases first to \dot{Q}_2 then to \dot{Q}_3 . So, by the time the flow signature representing \dot{Q}_1 arrives at the target location, the flow behind it has been impacted by increasing HRRs. In the case of the example, after time t_{TR} , the fire intensity is part way between \dot{Q}_3 and \dot{Q}_4 . Also shown in the sketch are the quantities of interest at the target location corresponding to HRR levels \dot{Q}_2 , \dot{Q}_3 , and \dot{Q}_4 . Since disturbances travel faster the higher the HRR, the separation between these signals at the target location will be smaller than Δt , in other words: $\Delta t_1 < \Delta t_2 < \Delta t_3 \dots < \Delta t$.

The total transport time, t_{TR} , for the disturbance associated with HRR \dot{Q}_1 could be calculated by simply substituting that HRR value in Eqs. (4)/(5) and (19)/(20). Though simple, this approach would imply that a disturbance would travel to the measurement site at the speed associated with the value of HRR at the time when the disturbance is initiated. However, if the fire intensity changes during the disturbance transfer interval, the flow is being sped up or slowed down in response to the changes in plume and ceiling layer velocities associated with the changing HRR values.

In the general case illustrated by the example in Fig. 2, the transit time, t_{TR} , is greater than the time interval, Δt , after which the heat release rate of the fire is assumed to increase from \dot{Q}_1 to \dot{Q}_2 and higher. The stepwise change in travel velocity will be handled by introducing an average transport velocity, V_i , defined as:

$$V_i = s/t_{TRi} , \tag{21}$$

where t_{TRi} is the transit time required by the flow to cover distance s under the conditions of constant HRR held at the “i” level, i.e., \dot{Q}_i . Based on this estimated average velocity, during time Δt , the flow will cover distance, s_i :

$$s_i = V_i \Delta t = (s/t_{TRi}) \Delta t . \tag{22}$$

If all the travel segments associated with the successive HRR levels are assumed to be additive, the disturbance will reach the measurement station when the distances s_1 , s_2 , etc. add up to s . Or, after canceling out distance, s , from both sides of the formula:

$$\sum_{i=1}^{N-1} (\Delta t/t_{TRi}) + \alpha_N (\Delta t/t_{TRN}) = 1 . \tag{23}$$

The second term on the left-hand side of the equation accounts for the fact that the disturbance will arrive at the measurement destination after a fraction of the last Δt interval. The two constants, N and α_N , are the only unknowns in the equation and they are chosen so that N is the largest integer that satisfies Eq. (23) with a value of α_N between 0 and 1. (For the case of the example in Fig. 2, it would be $N = 3$.) The total transport time is then calculated from:

$$t_{TR} = (N - 1 + \alpha_N) \Delta t . \tag{24}$$

Case of ceiling layer measurements

In the case where data on properties of the thermal environment produced by the fire are used to calculate the HRR evolution in time, the input information is typically provided by gas temperature measurements obtained in the ceiling layer. The correlations detailed in Ref. [2] or similar source can then be used to associate to each measurement the corresponding steady-state HRR value, as shown in the top plot of Fig. 3. The measured values are equally spaced in time, since data are

usually acquired at a fixed scan rate ($1/\Delta t$ in the diagram). However, in the time reference of the fire, the corresponding values are not equally spaced, since disturbances travel faster the higher the HRR. For example, for increasing HRR values, it will be $\Delta t_1 > \Delta t_2 > \Delta t_3$, etc. The challenge is to place the measurement station recordings (top diagram) on the time scale of the fire (bottom diagram).

The treatment is the same as that introduced to deal with the direct problem in the previous section. This time, however, the spacing of the HRR points in the fire time scale varies from scan to scan. Therefore, Eqs. (22) and (23) are now rewritten with the known Δt replaced by the unknown Δt_i s:

$$s_i = V_i \Delta t_i = (s/t_{TRi}) \Delta t_i \quad (25)$$

and

$$\sum_{i=1}^{N-1} (\Delta t_i / t_{TRi}) + \alpha_N (\Delta t_N / t_{TRN}) = 1 \quad (26)$$

Unlike the case involving known HRR values (cf., Eq. (23)), the above equation cannot be solved easily, since the time intervals, Δt_i , are unknown and not equal. While it may be possible to calculate the Δt_i values through a more complex model, possibly involving an iterative process, a simpler approach has been found suitable and is adopted here.

Consider the case where the disturbance corresponding to \dot{Q}_1 reaches the measurement station before HRR increases from \dot{Q}_1 to \dot{Q}_2 , i.e., $\Delta t_1 > t_{TR1}$. Further assume that the disturbance corresponding to \dot{Q}_2 arrives at the measurement station in a time shorter than Δt , namely $\Delta t > t_{TR2}$. The situation is depicted schematically in Fig. 4. In this scenario, the following equality applies:

$$t_{TR1} + \Delta t = \Delta t_1 + t_{TR2} \quad (27)$$

or

$$\Delta t_1 = \Delta t + t_{TR1} - t_{TR2} \quad (28)$$

The above equation can be generalized to:

$$\Delta t_i = \Delta t + t_{TRi} - t_{TRi+1} \quad (29)$$

Equation (29) can be substituted in Eq. (26), yielding:

$$\sum_{i=1}^{N-1} \frac{\Delta t + t_{TRi} - t_{TRi+1}}{t_{TRi}} + \alpha_N \frac{\Delta t + t_{TRN} - t_{TRN+1}}{t_{TRN}} = 1 \quad (30)$$

Since all terms are known, the values of N and α_N can now be determined using the same criteria introduced earlier and the transport time is then calculated as:

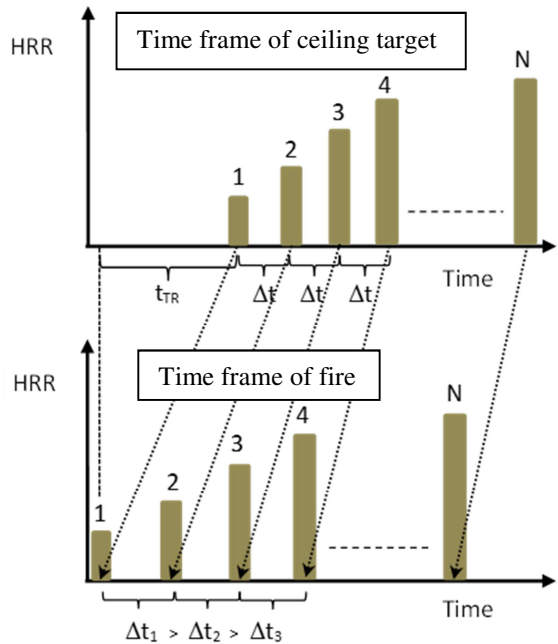


Fig. 3. Travel of disturbances during fire growth. Case of equally-spaced ceiling layer measurements (top).

$$t_{TR} = \sum_{i=1}^{N-1} \Delta t_i + \alpha_N \Delta t_N \quad (31)$$

After substitution of Eq. (29), the expression for the transit time, t_{TR} , becomes:

$$t_{TR} = (N - 1 + \alpha_N) \Delta t + (t_{TR1} - t_{TRN} + \alpha_N t_{TRN} - c \frac{HRR}{\dots}) \quad (32)$$

Implementation details

The time shifting of the HRR values inferred from the gas temperature measurements in the ceiling layer involves the following steps. The starting point is provided by the HRR values corresponding to the measured gas temperatures calculated at each time scan for the location where the measurement is available. The additional steps addressing the time shifting of those estimates are:

1. Using Eqs. (1)-(20), (30) and (32), calculate the total (plume + layer) transport time from the fire source to the measurement location, t_{TR} .
2. Enforce a lower limit (for example, based on a minimum temperature rise at the measurement location) for the minimum value of HRR to be used in the time shifting calculation.
3. Subtract the calculated transport time from the time corresponding to the data scan to obtain the corrected time for the HRR.
4. Complete steps 1-3 above for the entire data set.
5. Scan the sequence of corrected times to ensure that they are all in increasing order. Where this is not the case, replace the earlier time with an appropriate time, which is close to but greater than the previous scan time in the sequence.
6. By interpolation of the data shifted to the corrected times, determine the HRR values at the times of the original data scans.

Propagation at Low HRR Values

The above procedure has introduced the need to set a lower limit for the HRRs used to calculate transport times. Clear examples of situations that would otherwise be difficult to handle are those where the fire output either starts from zero or suddenly drops to zero. Under the extreme conditions of near-zero HRR the associated disturbance would take infinite time to propagate. More generally, very large travel times would be associated with very low HRRs. The solution selected here is to impose a minimum HRR threshold at each measurement point, corresponding to an assumed minimum temperature rise at that location, which was set equal to 2K. With this approach, the

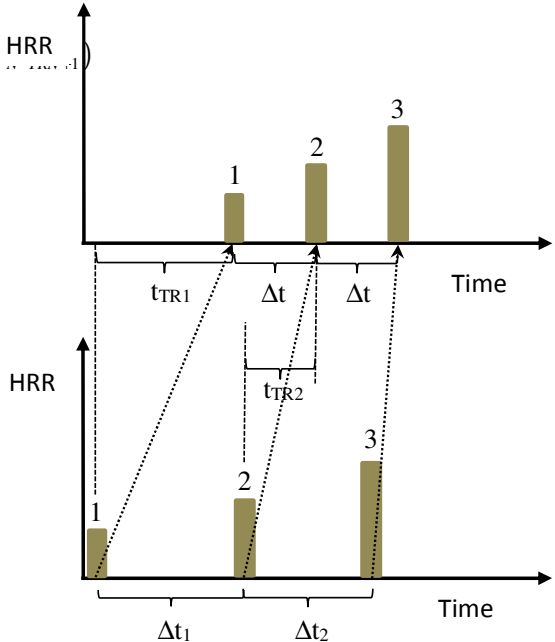


Fig. 4. Ideal case of disturbances traveling independent of each other.

transport time associated with the HRR threshold value is used whenever the HRR falls below this threshold. The practical impact of the approach will be discussed below when considering test data.

Flow Inertia Effects

The assumption that the flow promptly adapts to the HRR of the source was readily identified as a serious limitation. An example of the negative implications of this assumption is provided by the behavior of the model in the case of flow decay. As an extreme case, one can consider the situation where the source fire is suddenly turned off. Since $\dot{Q} = 0$ implies infinite travel time, the model as formulated would not allow the associated disturbance to ever propagate downstream, as was noted earlier. The solution to set a limit to the minimum value of HRR, while allowing for continuing propagation, still does not adequately account for the effect. The solution implemented here is to introduce an inertia term in the formula for the travel time.

The change in HRR from one level to another, implies a change in the average flow velocity. For example, in the transition from level \dot{Q}_i to \dot{Q}_{i+1} the quasi-steady average velocity goes from V_i to V_{i+1} . However, because of the inertia of the gas column involved, only a fraction of the change from V_i to V_{i+1} can be realized, causing the velocity at $i+1$ to be V_{i+1}^* instead of V_{i+1} . The new velocity can be calculated assuming that the change is a fixed fraction of the maximum possible, or:

$$V_{i+1}^* = V_i + \gamma(V_{i+1} - V_i) = \gamma V_{i+1} + (1-\gamma)V_i \quad (33)$$

Since the average velocity is proportional to the inverse of travel time (cf. Eq. (21)), the above equation can be turned into an expression for the modified travel time, t_{TRi+1}^* :

$$t_{TRi+1}^* = \left(\frac{\gamma}{t_{TRi+1}} + \frac{1-\gamma}{t_{TRi}^*} \right)^{-1} \quad (34)$$

In the application of this relaxation formula, it was found that use of the same value for the relaxation factor, γ would not achieve consistent results for HRR estimates during fire growth and for the portion of the data set characterized by rapid decrease in HRR. As a simple solution for the observed discrepancy, different values for the relaxation factor, γ were selected in the case of increasing or decreasing HRR: a value closer to 1 in the former case, closer to 0 in the latter. In addition to being attractively straightforward to implement, this approach enjoys qualitative support from the idea that an increase in the intensity of the fire causes the plume/ceiling layer momentum to readily increase due to the added buoyancy. On the other hand, when buoyancy decreases due to a drop in HRR, the flow responds more gradually to the corresponding driving force reduction. In practice, this hypothesis was successfully tested by setting:

$$\begin{aligned} \gamma^+ &= 0.5 && \text{for } \dot{Q}_{i+1} \geq \dot{Q}_i \text{ and} \\ \gamma^- &= 0.05 && \text{for } \dot{Q}_{i+1} < \dot{Q}_i \end{aligned} \quad (35)$$

EVALUATION OF CORRECTED HRR ESTIMATES

The performance of the correction method, which was evaluated by using unpublished data from large-scale fire tests, is presented in the following sections.

Three tiers of CEP (PS food trays) under 30-ft ceiling

The first condition considered to evaluate the time shifting method was introduced as the example case shown in Fig. 5. It refers to a fire test with three tiers (4.3-m [14-ft] high) of CEP commodity

under a 9.1-m (30-ft) ceiling. (CEP (Cartoned Expanded Plastic) is an acronym, which describes a standard commodity consisting of polystyrene food trays packaged in corrugated board boxes.) The application of the time shift to the HRR estimates is presented in Fig. 5a and 5b (uncorrected and corrected values, respectively). As can be seen, the consistency of the HRR estimates from the thermocouples of the five rings becomes very good after the time shift is applied. For these conditions, the 2K threshold implies lower HRR limits of 6 and 28 kW on average for Group 1 and Group 5 thermocouples, respectively. These HRR values can be interpreted as representing the HRR sensitivity limits associated with temperature measurements at varying distances from the fire axis. However, the corrected curves (Fig. 5b) would imply that HRRs can be resolved down to kW levels in the single digits. This is a particularly favorable result, which should not be generally expected, as will be seen in the examples to follow.

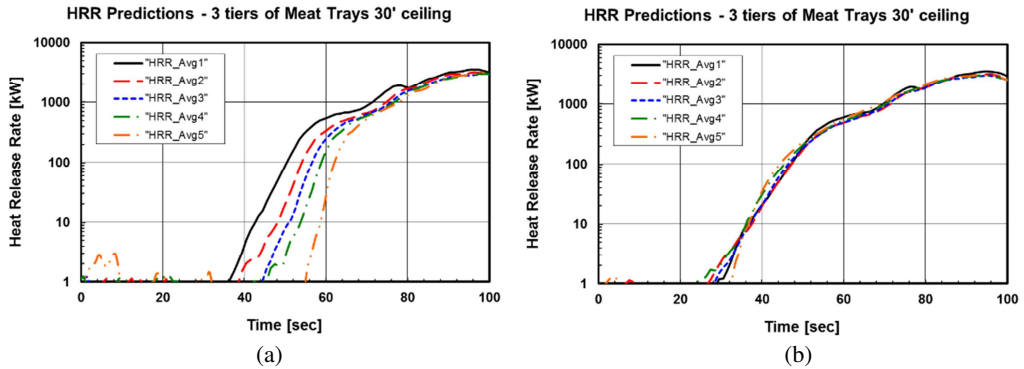


Fig. 5. Estimates of initial fire growth without (a) and with (b) time shifting correction. Plotted channels represent HRR averages calculated for five zones, with groups of thermocouples at varying distances from the fire axis. Data from a test for a 4.3-m (14-ft) array of Cartoned Expanded Plastic (CEP) under a 9.1-m (30-ft) ceiling.

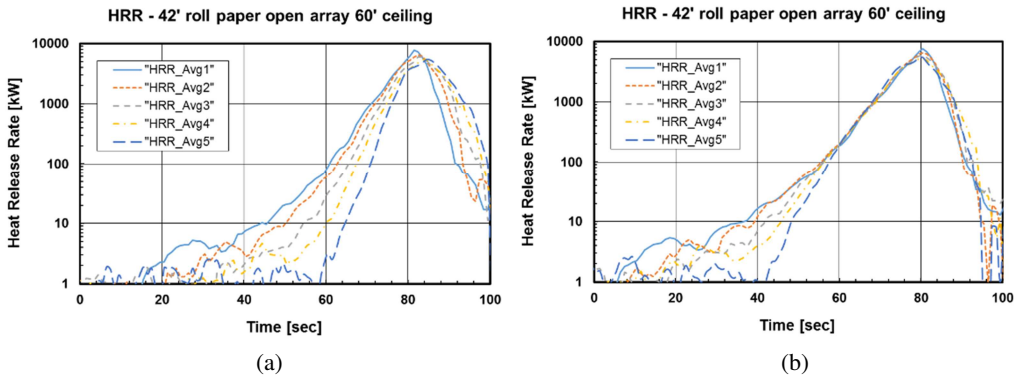


Fig. 6. Estimates of initial fire growth without (a) and with (b) time shifting correction. Plotted channels represent HRR averages calculated for five zones, with groups of thermocouples at varying distances from the fire axis. Data from a test for a 12.8-m (42-ft) open array of roll paper under an 18.3-m (60-ft) ceiling.

Roll paper 42-ft high under 60-ft ceiling

The second example used to validate the time shifting algorithm is from a fire with a tall roll paper array (12.8-m [42-ft] high) under an 18.3-m (60-ft) ceiling. This test provides another good case because of the very rapid rate of fire growth in this commodity. The HRR values with corrected

times are shown in Fig. 6b. As can be seen, the consistency among the HRR estimates is greatly improved compared to the uncorrected data (Fig. 6a), particularly above 100 kW. For this configuration, the 2 K threshold implies lower HRR limits of 13 and 62 kW on average for Group 1 and Group 5 TCs, respectively. In this case, the positive effect of the correction can also be observed in the decay portion of the fire. Also, the lower limit for resolving HRRs appears to be well above 10 kW, probably closer to 50-75 kW.

Heptane pool fire 44-in. Diameter under 23.4-ft ceiling

The last example involves the case of a heptane fire with a 1.1-m (44-in.) diameter pan under a ceiling 7.1 m (23.4 ft) above the pool surface. This is a particularly challenging situation, because the HRR increase after ignition is very rapid, owing to the relatively short transient to steady-state burning of this low boiling point fuel. The result of the application of the time shifting correction is shown in Fig. 7 for the growth portion of the test. As in the previous cases, the correction performs well in significantly reducing the discrepancy among the different HRR curves. For this geometry, the 2K threshold implies lower HRR limits of 8 and 36 kW on average for Group 1 and Group 5 TCs, respectively. Clearly, HRRs can only be properly resolved down to about 10 kW.

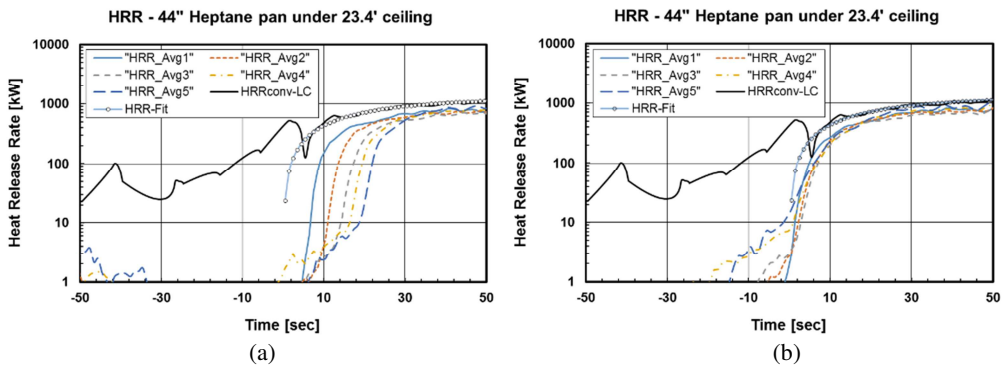


Fig. 7. Estimates of fire growth without (a) and with (b) time shifting correction. Plotted channels represent HRR averages calculated for five zones, with groups of thermocouples at varying distances from the fire axis. HRR estimate based on load cell data is also shown. Data from a test for a 1.1-m (44-in.) diameter heptane pool under a 7.1-m (23.4-ft) ceiling.

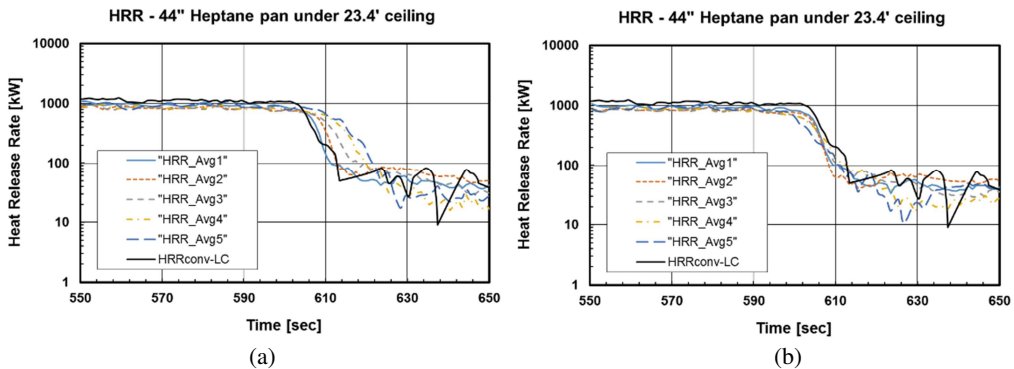


Fig. 8. Estimates of fire decay without (a) and with (b) time shifting correction. Plotted channels represent HRR averages calculated for five zones, with groups of thermocouples at varying distances from the fire axis. HRR estimate based on load cell data is also shown. Data from a test for a 1.1-m (44-in.) diameter heptane pool under a 7.1-m (23.4-ft) ceiling.

One additional curve is shown in the two plots of the figure as a solid black line labeled “HRRconv-LC”. It presents an estimate of the convective HRR based on load cell measurements of fuel consumption rate and assumed values for combustion efficiency (0.92) and convective fraction (0.68). At the start of the test, the load cell signal was disturbed by the ignition process, a fact that is apparent in a plot (not shown here) of the direct reading from this instrument. The issue explains the large values of HRR implied by these data between -50 and 10 sec. If the load cell readings are fitted starting at $t = 0$ and the fit is then used to calculate the HRR, the result is the line with the open circles labeled “HRR-Fit”. This curve is well behaved and provides a better description of the initial fire growth.

HRR plots for the decay phase at the tail end of the experiment are shown in Fig. 8. Here again, the time shifting correction is successful at bringing the curves from the different groups together. Also shown in the plot is the HRR estimate based on the load cell measurements. In this case, the data are not affected by spurious noise as the fire was allowed to decay undisturbed.

CONCLUSIONS

The paper has introduced a formalism to correct estimates of convective heat release rate (HRR) to account for travel time from the fire to the location of gas temperature measurements. The effect of the correction is to largely eliminate the dependence of these estimates on travel distance, a result that is necessary to provide accurate time resolution of rapidly changing fires. Though there are physical limits to the use of remote flow diagnostics, the proposed correction method greatly improves the analysis of data from large-scale fires. Similar benefits could be derived in other fire-related applications, such as the assessment of detection devices which rely on the sensing of transported flow properties (smoke, temperatures, trace compounds).

ACKNOWLEDGMENTS

Karl Meredith, Prateep Chatterjee and Lou Gritzo, all with FM Global Research, critically reviewed an early internal document on this work and provided useful suggestions, which have been largely incorporated. I am grateful for the time and attention that they devoted to the task.

REFERENCES

- [1] F. Tamanini, Heat Release Rate and Sprinkler Response Characterization in Large-Scale Fires, Proc. of the Sixth International Seminar on Fire and Explosion Hazards, Edited by D. Bradley, G. Makhviladze and V. Molkov, 2011, pp. 330-341.
- [2] F. Tamanini, Fire Plume and Ceiling Layer Correlations and Their Merging, FM Global Research Technical Report, Project ID RW000078, August 2018. Available from: <https://www.fmglobal.com/research-and-resources/research-and-testing/research-technical-reports>
- [3] H-Z Yu, Transient Plume Influence in Measurement of Convective Heat Release Rates of Fast-Growing Fires Using a Large-scale Fire Products Collector, J. of Heat Transfer, Transactions of the ASME, 112 (1990) 186-191.
- [4] K. Nitta, Y. Oka, J. Yamaguchi, K. Muraoka, R. Mase, Prediction of Heat Release Rate Based on Ceiling Jet Temperature in Case of Time-dependent Fire, In: Fire Safety Science–Proceedings of the Ninth International Symposium, pp. 813-824, 2018.